HIGH-RESOLUTION SPECTROSCOPY
ON THE B²Σ⁺, v'=0←X²Π, v"=1 TRANSITION IN SiCl

Gerard MEIJER, Bob JANSEN, J.J. TER MEULEN and A. DYMANUS

Department of Molecular and Laser Physics, Katholieke Universiteit Nijmegen,
Toernooiveld, 6525 ED Nijmegen, The Netherlands

High-resolution laser-induced fluorescence spectra of $^{28}Si^{35}Cl$ and $^{28}Si^{37}Cl$ have been observed in a molecular beam. Accurate constants describing the rotational structure in the X²Π, $v"=1$ as well as in the electronically excited B²Σ⁺, $v'=0$ state are given. An inverted fine structure was found in the excited state with a spin-splitting constant $\gamma = -31.15 \pm 0.19$ MHz for $Si^{35}Cl$ and $\gamma = -30.62 \pm 0.61$ MHz for $Si^{37}Cl$.

1. Introduction

The SiCl radical (chlorosilylidyne) is an important reaction product in the chemical etching process of silicon-containing compounds by chlorine. Laser-induced fluorescence (LIF) via the strong B←X transition in the 285–305 nm range is perfectly suited to probe concentrations and internal state distributions of the SiCl radicals produced in these processes. In this field there is great interest in detailed spectroscopic data on this radical.

Electronic spectra of the SiCl radical were first observed by Jevons [1] in 1913. Jevons [2] analysed in 1936 several ultraviolet band systems of SiCl, including the measurements carried out by Datta [3]. Although the identification of the observed band heads was not correct, the electronic nature of the X²Π and the B²Σ state was correctly identified. The difficulties experienced by Jevons in assigning some bands at the short wavelength side of the B→X system were solved many years later (1964) by Verma, who attributed these bands to the B'²Δ→X²Π transition [4].

The first rotational analysis of three vibrational bands of the B→X system was performed by Ovcharenko et al. [5], who characterized the B state as a ²Σ⁺ state. Mishra and Khanna [6] re-photographed the same system and observed more vibrational bands enabling them to improve the vibrational constants. They also performed a rotational analysis of some bands in the B²Σ⁺→X²Π₃/₂ subsystem and predicted an appreciable spin splitting in the excited state, with a splitting constant $\gamma = 0.0098$ cm⁻¹. Rai et al. [7] showed, however, this value to be incorrect due to a misinterpretation of $Si^{37}Cl$ isotopic lines as lines of a satellite branch.

Bredohl and co-workers have carried out a series of extensive studies on the A→X, B→X, C→X, D→X, E→X and F→X transitions of SiCl [8–11]. From these studies the nature of the electronic states was clarified, and accurate rotational and vibrational constants were obtained. An analysis of rotational and hyperfine structure in the microwave spectrum of $Si^{35}Cl$ in the X²Π, $v"=0$ state has been undertaken recently by Tanimoto et al. [12].

In the present study high resolution LIF spectra of SiCl originating from the B²Σ⁺, $v'=0←X²Π$, $v"=1$ transition are observed in a molecular beam. From an analysis of these spectra the rotational structure in both electronic states, including the resolved spin splitting in the B²Σ⁺ state, could be determined with a higher accuracy than in previous measurements. Both isotopic species, $^{28}Si^{35}Cl$ and $^{28}Si^{37}Cl$, were observed in a ratio of 3:1 (natural abundance). As lines of both isotopes are measured in continuous single mode scans of our

laser, the isotope splitting could be determined with high precision. Very accurate positions of the band heads are given, for both $Si^{35}Cl$ and $Si^{37}Cl$ which, for the $0 \leftarrow 1$ band studied, has band heads in regions of strong lines from the more abundant $Si^{35}Cl$ isotope.

2. Experimental

The SiCl radicals are produced in a microwave discharge (100 W at 2.45 GHz) in a flowing gas mixture of about 10% $SiCl_4$ in 10 mbar Ar. We used a coaxial microwave discharge tube, which has been described previously [13]. The discharge in pure Ar gives a bright pink-red flame. When a small amount of $SiCl_4$ is added the colour of the flame changes to blue; best SiCl signals were observed when the flame had a whitish glow. Under optimum production conditions there is considerable UV light from the production zone, which gives a relatively large fluorescence background in our LIF experiment. This background UV fluorescence mainly arises from the $SiCl_2(\tilde{A}\,^1B_1 \leftrightarrow \tilde{X}\,^1A_1)$ transition [14], and could be suppressed using an Hg 289 nm interference filter. The presence of $SiCl_2$ radicals in the beam has been verified by the observation of the very intense $SiCl_2(\tilde{A}\,^1B_1 \leftarrow \tilde{X}\,^1A_1)$ LIF spectra in the 315–330 nm range. A part of one of these complex but completely resolved spectra is shown in fig. 1.

At the inner side of the pyrex glass tube in which the discharge takes place and also on the molecular beam orifice a deposit of polymeric $(SiCl_2)_n$ is formed. This polymerisation is thought to be the main reason for the occurrence of instabilities in the discharge after several hours of operation. The radical source is mounted only a few mm away from the beam orifice, which is formed by a 2 mm hole in a boron nitride plate. This large hole diameter was chosen in order to prevent clogging by the polymeric $(SiCl_2)_n$.

The molecular beam generator, the UV production and the LIF detection zone have been described earlier [13,15], and only a brief summary is given here. Detection of SiCl radicals is carried out by means of LIF, in a region about 15 cm downstream from the beam orifice. The SiCl radicals in the $X\,^2\Pi$, $v''=1$ state are excited to the $B\,^2\Sigma^+$, $v'=0$ state with narrow-band tunable UV radiation in the $\lambda = 296$–299 nm range. Total fluorescence from this state back to the ground state is detected. The UV radiation is obtained by frequency doubling in a $LiIO_3$ crystal inside the cavity of a single-frequency ring-dye laser, operating on rhodamine 6G. Although self-absorption of the doubling crystal becomes important at wavelengths below 300 nm, it was still possible to obtain 1–2 mW tunable UV radiation with a bandwidth of about 0.5 MHz (rms), by pumping the

$SiCl_2\,(\tilde{A}\,^1B_1 \leftarrow \tilde{X}\,^1A_1)$
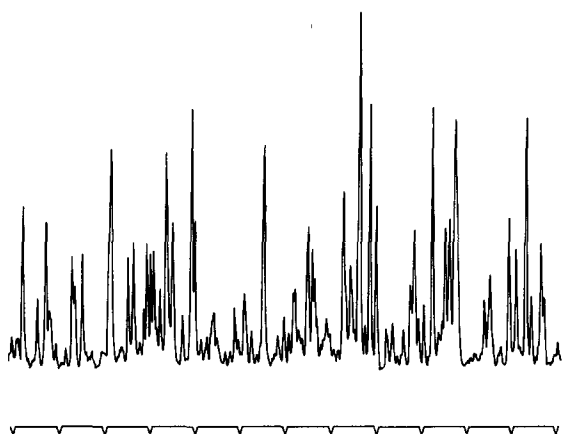
Fig. 1. Recording of a part of the $SiCl_2(\tilde{A}\,^1B_1 \leftarrow \tilde{X}\,^1A_1)$ LIF spectrum around 324 nm. The distance between the interferometer markers, lower trace, is 598.82 ± 0.04 MHz. Beam production conditions are the same as for SiCl.

dye laser with 5 W of an Ar ion laser (all lines). Unfortunately we could not produce sufficient UV in the 292–294 nm region to excite SiCl from its electronic and vibrational ground state. As the Franck–Condon factors for the $v' = 0 \leftarrow v'' = 0$ and the $v' = 0 \leftarrow v'' = 1$ transitions are nearly equal [16], detection of SiCl via the $v' = 0 \leftarrow v'' = 1$ transition is less efficient only because of a lower population of the $v'' = 1$ state. The SiCl radicals are, however, produced rotationally hot; from the LIF spectra a rotational temperature of about $T_R = 800$ K is found. If the same temperature is assumed for the vibrational distribution, this means that about 25% of the SiCl radicals are produced in the $v'' = 1$ state. This state lives long enough to reach the detection zone.

The spectra were recorded together with the markers of a pressure and temperature stabilized interferometer with a free spectral range of 299.41 ± 0.02 MHz. This enabled us to measure splittings between different rotational transitions with an accuracy of about 30 MHz. For absolute frequency measurements the absorption spectrum of I_2 vapour in a cell at the fundamental laser frequency was measured. The correction to the wavelengths in the I_2 atlas of -0.0056 cm^{-1} was taken into account [17]. The estimated error in the absolute frequencies is ≈ 150 MHz, due to the drift of the interferometer and particularly due to the inaccuracy in the determination of the centre of the broad and not always symmetric I_2 lines.

3. Theory

For the description of the energy levels in the X $^2\Pi$ ground state, we use the Hamiltonian

$$H = B''(R^2) - D''(R^2)^2 + \gamma'' N \cdot S + A'' L \cdot S + \tfrac{1}{2} A_D''[(R^2)(L \cdot S) + (L \cdot S)(R^2)] \tag{1}$$

with S and L the electronic spin and orbital angular momentum, respectively, $N = J - S$ with J the total rotational angular momentum of the molecule and $R = J - L - S$, the end-over-end rotational angular momentum of the nuclei. The Hamiltonian (1) describes the rotational and spin–orbit energy including first-order centrifugal distortion contributions, Λ doubling and spin–rotation interactions [18]. Since the ground state of SiCl is almost pure Hund's case (a) ($A''/B'' \approx 815$) we work in the J^2 formalism. The basis functions we use are symmetrized Hund's case (a) wavefunctions, defined as:

$$|^2\Pi_\Omega, JM \pm \rangle = 2^{-1/2}(|^2\Pi_\Omega, JM\rangle \pm |^2\Pi_{-\Omega}, JM\rangle) . \tag{2}$$

In this basis set $\{|^2\Pi_{1/2}, JM \pm \rangle; |^2\Pi_{3/2}, JM \pm \rangle\}$ the Hamiltonian matrix can be written in the form

$$(H) = B'' \begin{bmatrix} Z+1 & -Z^{1/2} \\ -Z^{1/2} & Z-1 \end{bmatrix} + A'' \begin{bmatrix} -\tfrac{1}{2} & 0 \\ 0 & \tfrac{1}{2} \end{bmatrix} - D'' \begin{bmatrix} (Z+1)^2 + Z & -2Z^{3/2} \\ -2Z^{3/2} & (Z-1)^2 + Z \end{bmatrix}$$

$$+ \tfrac{1}{2} A_D'' \begin{bmatrix} -(Z+1) & 0 \\ 0 & Z-1 \end{bmatrix} + \gamma'' \begin{bmatrix} -1 & \tfrac{1}{2} Z^{1/2} \\ \tfrac{1}{2} Z^{1/2} & 0 \end{bmatrix} \mp (J + \tfrac{1}{2}) \begin{bmatrix} \tfrac{1}{2}p + q & -\tfrac{1}{2}q Z^{1/2} \\ -\tfrac{1}{2}q Z^{1/2} & 0 \end{bmatrix}$$

$$+ \begin{bmatrix} \tfrac{1}{2}q^*(Z+2) + \tfrac{1}{2}p^* + o & -\tfrac{1}{2}(\tfrac{1}{2}p^* + q^*)Z^{1/2} \\ -\tfrac{1}{2}(\tfrac{1}{2}p^* + q^*)Z^{1/2} & \tfrac{1}{2}q^* Z \end{bmatrix}, \tag{3}$$

where $Z = (J - \tfrac{1}{2})(J + \tfrac{3}{2})$.

The rotational (B'', D''), spin–orbit (A'', A_D'') and spin–rotation (γ'') constants are defined as by Zare et al. [19], while the Λ-doubling constants (p, q, p^*, q^* and o) are defined as in the original work of Mulliken and Christy [20]. An independent determination of the molecular constants of eq. (3) is not possible as a consequence of the correlation between the molecular constants. As shown by Brown and Watson [21], A_D'' and γ'' in particular are nearly totally correlated. These correlations can be removed in the following manner. First we diagonalize a Hamiltonian H_0, which comprises only the first two terms of (3). Using the resultant eigenfunctions the matrix elements of the complete Hamiltonian (1) are calculated. The correlations are removed

by collecting terms with the same functional dependence and introducing new effective molecular constants:

$$B''_{eff} = B'' + \tfrac{1}{2}q^* ,$$

$$A''_{eff} = A'' - o + A''_D \frac{A'' - 2B''}{2B''} ,$$

$$\gamma''_{eff} = \gamma'' - \tfrac{1}{2}p^* - A''_D \frac{A'' - 2B''}{2B''} . \tag{4}$$

When expressed in these effective constants the Hamiltonian matrix based on the eigenfunctions (2) is, in the approximation $A''/B'' \gg 1$.

$$[H] = B''_{eff} \begin{bmatrix} Z+1 & -Z^{1/2} \\ -Z^{1/2} & Z-1 \end{bmatrix} + A''_{eff} \begin{bmatrix} -\tfrac{1}{2} & 0 \\ 0 & \tfrac{1}{2} \end{bmatrix} - D'' \begin{bmatrix} (Z+1)^2 + Z & -2Z^{3/2} \\ -2Z^{3/2} & (Z-1)^2 + Z \end{bmatrix}$$

$$+ \gamma''_{eff} \begin{bmatrix} -1 & \tfrac{1}{2}Z^{1/2} \\ \tfrac{1}{2}Z^{1/2} & 0 \end{bmatrix} \mp (J+\tfrac{1}{2}) \begin{bmatrix} \tfrac{1}{2}p+q & -\tfrac{1}{2}qZ^{1/2} \\ -\tfrac{1}{2}qZ^{1/2} & 0 \end{bmatrix} + k \begin{bmatrix} 1 & 0 \\ 0 & 1 \end{bmatrix} ,$$

with $k = \tfrac{1}{2}(q^* + o) - \tfrac{1}{4}(A''/B'')A''_D$.

A different approach to the correlation problem is to include the effect of γ'' in the other constants and to use instead a term equal to

$$\tfrac{1}{2}A''_{D,eff} \begin{bmatrix} -(Z+1) & 0 \\ 0 & Z-1 \end{bmatrix} .$$

In this case also A''_{eff} and k change, and we get

$$A''_{eff} = A'' - o + \gamma'' - \tfrac{1}{2}p^* ,$$

$$A''_{D,eff} = A''_D - (\gamma'' - \tfrac{1}{2}p^*) \frac{2B''}{A'' - 2B''} ,$$

$$k = \tfrac{1}{2}(q^* + o) - (\gamma'' - \tfrac{1}{2}p^*) \frac{A''}{2(A'' - 2B'')} . \tag{6}$$

For the excited B $^2\Sigma^+$ state we use the Hamiltonian in the N^2 formalism, appropriate for Hund's case (b):

$$H = B'(N^2) - D'(N^2)^2 + \gamma' N \cdot S . \tag{7}$$

Higher-order centrifugal distortion or spin–rotation effects are smaller than the precision of the present measurements and were not included in the analysis.

The chlorine nucleus has a nuclear spin $I = 3/2$, and so there are contributions to the Hamiltonians (1) and (7) from hyperfine interactions. The magnitude of the hyperfine splitting in both the B $^2\Sigma^+$, $v' = 0$ and the X $^2\Pi$, $v'' = 1$ state is not known, but a first approximation for the splitting in the latter state can be made by assuming the same magnetic hyperfine (a, b, c and d) and electric quadrupole (eQq_1) coupling constants as for the X $^2\Pi$, $v'' = 0$ state of Si^{35}Cl obtained by Tanimoto et al. [12]. It is found that for the large values of J'' relevant in the present experiment only d and eQq_1 can produce a significant splitting; the contributions of a, b and c are inversely proportional to J'' and can be disregarded. From these two interactions we calculate a total hyperfine splitting in the $^2\Pi_{1/2}$ and $^2\Pi_{3/2}$ states of about 70 and 6 MHz, respectively. In all transitions recorded no clear splitting due to hyperfine structure has been observed. This indicates that hyperfine splittings in the excited electronic state are of the same order as those in the ground state. Careful analysis of some of

the lineshapes suggests that these could be envelopes of transitions between hyperfine sublevels. If this is assumed then the linewidths and lineshapes can be explained from the hyperfine splitting in the ground state only. This indicates (albeit not conclusively) that the hyperfine splittings in the excited state are smaller than in the ground state. Consequently we felt justified in disregarding hyperfine structure in the excited state within the limited resolution of the present experiment.

4. Results and discussion

A typical example of a fast "overview" laser scan is given in fig. 2. The observed LIF spectrum is shown together with the reference absorption spectrum of I_2 and the transmission peaks of the interferometer. The band head for the P_2 transitions of the most abundant $Si^{35}Cl$ isotope and several lines of the $^OP_{12}$ branches of both isotopes can clearly be seen. Even for low values of the quantum number N', the ρ doubling in the P_2 branch is resolved as shown in fig. 3, recorded at a slower laser scan. As the ground state is an almost pure Hund's case (a) state, line intensities are almost independent of the ΔN selection rules [22], and the satellite lines $^PQ_{12}(N)$ are even stronger than the main $P_2(N)$ lines. From the intensity ratio of subsequent P_2 transitions the SiCl is seen to be rotationally hot. Maximum signals occur for J'' between 28.5 and 35.5, which indicates a rotational temperature of about 800 K.
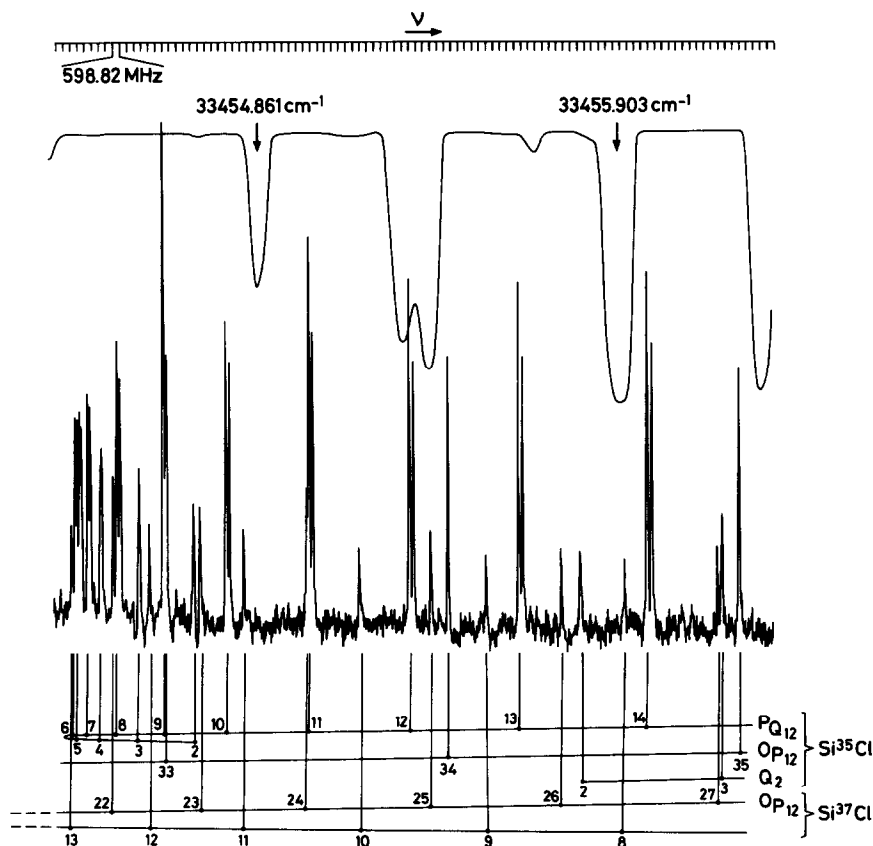
Fig. 2. Recording of a part of the B $^2\Sigma^+$, $v'=0 \leftarrow$ X $^2\Pi$, $v''=1$ LIF spectrum of SiCl in a 60 GHz continuous scan of the laser. From the resolved ρ doublets, consisting of $P_2(N)$ and $^PQ_{12}(N)$ lines, only the stronger $^PQ_{12}(N)$ lines are indicated.
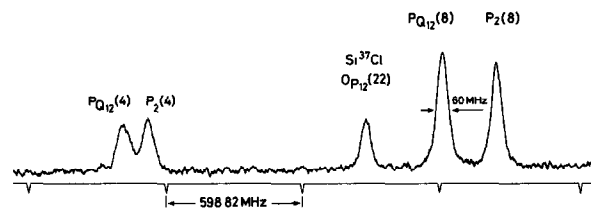
Fig. 3. Part of the spectrum of fig. 2, recorded at a slower laser scan. The stronger $^PQ_{12}(N)$ lines lie lower in frequency than the corresponding $P_2(N)$ lines which includes an inverted fine structure in the B $^2\Sigma^+$, $v'=0$ state. The observed linewidth of about 60 MHz is mainly caused by residual Doppler broadening in the molecular beam.

As shown in fig. 3 the full width at half maximum of the spectral lines starting from the $X\,^2\Pi_{3/2}$ multiplet is about 60 MHz, mostly due to residual Doppler broadening caused by the divergence of the molecular beam. The lines from the $X\,^2\Pi_{1/2}$ multiplet are broader (about 120 MHz) and show a more or less flat maximum. This can be explained by the larger hyperfine splitting in the $^2\Pi_{1/2}$ multiplet (section 3). Line positions are determined by taking the center of a Gaussian profile with the same full width at half maximum as the observed line.

For the determination of the rotational structure we first measured the spin splitting in the B $^2\Sigma^+$ state. This is determined by the last term of the Hamiltonian (7), and is equal to $\gamma'(N'+\tfrac{1}{2})$. As can be seen directly from each individual p doublet, and as follows also from the fit of the total spectrum, the γ' constant is negative. This means that the fine structure in the B $^2\Sigma^+$ state is inverted. The value of the γ' constant follows from a least-squares fit of the observed spin splitting for 22 values of N' to the expression $\gamma'(N+\tfrac{1}{2})$. Even for N' values up to $N'=55$ no significant deviation from linear behaviour was found. We obtained $\gamma'=-31.15\pm0.19$ MHz, where the error corresponds to one standard deviation. This value of γ' was fixed when fitting the other constants.

In the pure precession approximation [23] a several times larger but negative value for the spin-splitting constant is expected if only the interaction of the B $^2\Sigma^+$ state with the $X\,^2\Pi$ ground state is considered. There are however, two other $^2\Pi$ states lying just above the B $^2\Sigma^+$ state. Because of the smaller value for the spin-orbit coupling constants (A) in these states [10], the interaction with these states is not strong enough to invert the sign of the spin splitting in the B $^2\Sigma^+$ state, although it cancels the interaction with the $X\,^2\Pi$ ground state to a large extent.

Table 1
Effective molecular constants (in cm^{-1}) for the $X\,^2\Pi$, $v''=1$ and the B $^2\Sigma^+$, $v'=0$ state of $Si^{35}Cl$ and $Si^{37}Cl$, obtained from a least-squares fit to eqs. (4) and (5). Values in parentheses are one standard deviation

Constant	$Si^{35}Cl$		$Si^{37}Cl$	
	present study	ref. [9]	present study	ref. [9]
ν_{01}	33558.0296(7)	33558.03	33563.2919(18)	33563.32
B''_{eff}	0.253793(15)	0.253789(46)	0.24757(11)	0.24779(14)
$10^6 D''$	0.2678(43)	0.2270(76)	0.19(11)	0.229(26)
A''_{eff}	206.8062(12)	206.786(11)	206.8122(22)	206.797(26)
γ''_{eff}	0.02221(23)		0.0232(18)	
$10^3(p+2q)$	4.545(33)		4.42(23)	3.91(82)
$10^3 p$	4.478(33)	4.37(30)		
$10^5 q$	3.37(64)			
$\Delta B \equiv B' - B''_{eff}$	0.0244831(10)		0.0238682(74)	
B'	0.278276(16)	0.278267(46)	0.27143(12)	0.27165(14)
$10^6 \Delta D \equiv 10^6(D'-D'')$	$-0.05560(37)$		$-0.062(14)$	
$10^6 D'$	0.2122(35)	0.1690(79)	0.12(8)	0.172(23)
$10^3 \gamma'$	$-1.039(7)$		$-1.021(20)$	

Table 2
Position of the band heads (in cm^{-1}) for the B $^2\Sigma^+$, $v'=0\leftarrow$X $^2\Pi$, $v''=1$ transition of Si^{35}Cl and Si^{37}Cl

Band head	Si^{35}Cl		Si^{37}Cl	
	observed	calculated	observed	calculated
P$_1$; P$_1$(16)	33655.0186(50)	33655.0179	33660.4335(50)	33660.4347
Q$_1$; Q$_1$(5)	33660.6634(50)	33660.6606	33665.9421(50)	33665.9456
^{O}P$_{12}$; ^{O}P$_{12}$(17)		33448.4944		33453.9015
P$_2$; ^{P}Q$_{12}$(6)	33454.3315(50)	33454.3334	33459.6020(50) [a]	33459.5997

[a] ^{P}Q$_{12}$(6) is hidden under the Q$_2$(9) band of Si^{35}Cl.

Frequency differences between closely spaced rotational transitions as well as absolute frequencies of the rotational transitions of all the twelve possible branches were included in the input data set for the least-squares fit program. Since the electronic spectra are especially sensitive to differences between rotational constants we fitted B''_{eff}, $\Delta B \equiv B' - B''_{\text{eff}}$, D' and $\Delta D \equiv D' - D''$ rather than B''_{eff}, B', D'' and D'. We also fitted $p+2q$ and q instead of p and q separately. In total we included 60 frequency differences and 71 absolute frequencies. The highest J'' level we observed was the $J''=68.5$ via the P$_1$(68). All measured absolute frequencies and frequency differences fitted well within the experimental errors. The standard deviation of the overall fit was 30 MHz. The effective constants we obtained for Si^{35}Cl are tabulated in table 1. If our constants are compared with the values of Bredohl et al. [9], who used a similar Hamiltonian, we find a good agreement, except for the D constants for which we find significantly larger values. This discrepancy might be due to the fact that Bredohl et al. were unable to resolve the spin splitting in the excited state and also did not include the spin–rotation interaction in the ground state. The values of the effective constants, obtained when $A''_{D,\text{eff}}$ is fitted rather than γ''_{eff}, can be directly calculated from eq. (6). It should therefore be noted that the band origin ν_{01} includes the contribution of the last term in the Hamiltonian (5). In table 2 accurate positions of the band heads are given.

For the Si^{37}Cl isotope the same procedure was followed, giving a value of $\gamma' = -30.62 \pm 0.61$ MHz for the spin-splitting constant. In this case 33 frequency differences and 43 absolute frequencies were included in the fit of the spectrum. Since the highest J'' level included here was only the $J''=33.5$ the higher order constants of eq. (5) in particular were determined less accurately than for Si^{35}Cl. The effective constants we obtained and the positions of the band heads are given in tables 1 and 2.

Acknowledgement

References

[1] W. Jevons, Proc. Roy. Soc. A89 (1913) 187.
[2] W. Jevons, Proc. Phys. Soc. (London) 48 (1936) 563.
[3] A.C. Datta, Z. Physik 78 (1932) 486.
[4] R.D. Verma, Can. J. Phys. 42 (1964) 2345.
[5] I.E. Ovcharenko, L.N. Tunitskii and V.I. Yakutin, Opt. Spectry. 8 (1960) 393.
[6] R.K. Mishra and B.N. Knanna, Current Sci. 38 (1969) 361.
[7] S.B. Rai, J. Singh, K.N. Upadhya and D.K. Rai, J. Phys. B7 (1974) 415.

[8] H. Bredohl, I. Dubois, Y. Houbrechts and H. Leclerq, J. Phys. B11 (1978) L137.

[9] H. Bredohl, Ph. Demoulin, Y. Houbrechts and F. Mélen, J. Phys. B14 (1981) 1771.

[10] F. Mélen, Y. Houbrechts, I. Dubois, Bui Lê Huyên and H. Bredohl, J. Phys. B14 (1981) 3637.

[11] H. Bredohl, R. Cornet, I. Dubois and F. Mélen, J. Phys. B15 (1982) 727.

[12] M. Tanimoto, S. Saito, Y. Endo and E. Hirota, J. Mol. Spectry. 103 (1984) 330.

[13] W. Ubachs, J.J. ter Meulen and A. Dymanus, Can. J. Phys. 62 (1984) 1374.

[14] D. Sameith, J.P. Mönch, H.-J. Tiller and K. Schade, Chem. Phys. Letters 128 (1986) 483.

[15] W.A. Majewski, Opt. Commun. 45 (1983) 201.

[16] J. Singh and P.S. Dube, Indian J. Pure Appl. Phys. 9 (1971) 164.

[17] S. Gerstenkorn and P. Luc, Atlas du spectroscopie d'absorption de la molécule d'iode (CNRS, Paris, 1978); Rev. Phys. Appl. 14 (1979) 791.

[18] J.M. Brown, M. Kaise, C.M.L. Kerr and D.J. Milton, Mol. Phys. 36 (1978) 553.

[19] R.N. Zare, A.L. Schmeltekopf, W.J. Harrop and D.L. Albritton, J. Mol. Spectry. 46 (1973) 37.

[20] R.S. Mulliken and A. Christy, Phys. Rev. 38 (1931) 87.

[21] J.M. Brown and J.K.G. Watson, J. Mol. Spectry. 65 (1977) 65.

[22] G. Herzberg, Spectra of diatomic molecules (Van Nostrand, Princeton, 1950).

[23] J.H. van Vleck, Phys. Rev. 33 (1929) 467.